JOURNAL OF NATURAL PRODUCTS

Article

pubs.acs.org/jnp

Agarsenone, a Cadinane Sesquiterpenoid from *Commiphora erythraea*

Stefano Santoro,[†,§] Stefano Superchi,*[,‡] Federica Messina,[†] Ernesto Santoro,[‡] Ornelio Rosati,[†] Claudio Santi,[†] and M. Carla Marcotullio*[,†]

[†]Dipartimento di Chimica e Tecnologia del Farmaco-Sez. Chimica Organica, Università di Perugia, Via del Liceo, 1-06123 Perugia, Italy

[‡]Dipartimento di Scienze, Università della Basilicata, Viale dell'Ateneo Lucano, 10- 85100 Potenza, Italy

Supporting Information

ABSTRACT: Agarsenone (**1**), a new cadinane sesquiterpenoid, was isolated from the resin of *Commiphora erythraea*. The structures of **1** and its decomposition products agarsenolides (**2a** and **2b**) and myrrhone (**3**) were established by extensive NMR spectroscopic analysis. The absolute configuration of **3** and the relative and absolute configurations of **1** were assigned by comparison of experimental and calculated optical rotatory dispersion and electronic circular dichroism spectra.

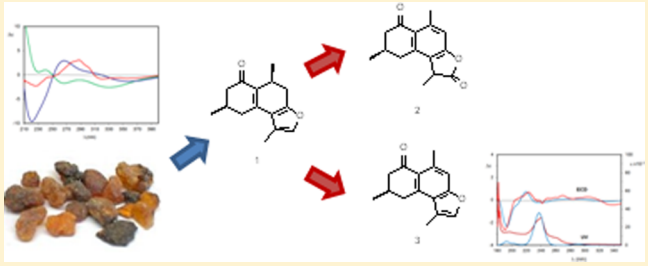

The genus *Commiphora* comprises more than 150 species and is known for the production of resin commonly called myrrh. *Commiphora erythraea* (Ehrenb.) Engl. (Burseraceae) is a small tree growing in the Arabian Peninsula and widespread in Ethiopia, where its resin (called agarsu) is used to protect livestock from ticks, to prevent colds and fever, to enhance wound healing, as an antimalarial, against snake venom poisoning, as an anti-inflammatory, as an antiseptic, and against skin infections.[1] The paucity of chemical data[2,3] about *C. erythraea* initiated our study of the composition of its resin.[4] Furanosesquiterpenoids with eudesmane, germacrane, elemane, or guaiane skeletons are the most abundant classes of metabolites of oils and extracts prepared from myrrh.[5,6]

In our previous studies of the resin extracts we identified four main known compounds, namely, 1,10(15)-furanogermacradien-6-one (**4**), 1(10),4-furanodien-6-one (**5**), *rel*-3*R*-methoxy-4*S*-furanogermacra-1*E*,10(15)-dien-6-one (**6**), and *rel*-2*R*-methoxy-4*R*-furanogermacra-1(10)*E*-en-6-one (**7**)[7,8] along with dihydropyrocurzerenone (**8**),[7] curzerenone (**9**),[7] myrrhone (**3**),[9,10] and alismol (**10**)[11] (Figure S1, Supporting Information). Compounds **4**−**7** and myrrhone (**3**) showed antiradical,[6] anti-inflammatory,[12] and antiviral activity.[13] A new investigation of the resin permitted the isolation of two known furanosesquiterpenoids (**11**[14] and **12**[15]) and a new furanocadinan-2-one, named agarsenone (**1**).

Herein, we report the isolation and structure elucidation of agarsenone (**1**) and its decomposition products, agarsenolides (**2a** and **2b**) and myrrhone (**3**). This work also illustrates a successful application of computational analysis of optical rotatory dispersion (ORD) and electronic circular dichroism (ECD) in determining the relative and absolute configuration of these noncrystalline natural products. In fact, in recent years, the use of computational techniques to calculate chiroptical properties has become an important tool for the assignment of absolute[16] and relative configurations.

RESULTS AND DISCUSSION

Agarsenone (**1**) was isolated as a colorless oil from the MeOH extract of the commercial resin. The HRMS of the quasi-molecular $[M + H]^+$ ion at m/z 231.1367 established the molecular formula $C_{15}H_{18}O_2$ for **1**, indicating seven indices of hydrogen deficiency, and the IR spectrum showed the presence of a conjugated carbonyl group (1762 cm^{-1}). ^1H NMR analysis in $CDCl_3$ revealed the presence of a furanosesquiterpenoid compound. During acquisition of NMR spectra, the compound partially decomposed, and TLC analysis, further confirmed by GC-MS, revealed the presence of a small amount of **1** along with **3**. After 48 h in $CDCl_3$ solution, compound **1** was completely transformed into **3**.

The stability of **1** in several solvents, such as $CHCl_3$, Et_2O, benzene, and *n*-hexane, was checked to find experimental conditions suitable to prevent its decomposition and to determine its structure. Compound **1** was found to be unstable only in $CHCl_3$ and in other chlorinated solvents.[17] No acidic degradation was observed on SiO_2, unless chlorinated solvents were used for the elution. NMR spectra were then recorded in benzene-d_6, allowing the determination of the agarsenone structure (Table 1). However, some coupling constants were taken from the ^1H NMR data in $CDCl_3$, which showed patterns more consistent with first-order spin systems (see Experimental Section).

The ^{13}C NMR spectrum of **1**, supported by a JMODXH experiment,[18] indicated one carbonyl, five nonprotonated sp^2

Received: February 5, 2013
Published: July 11, 2013

Table 1. NMR Data for Compounds 1 and 2[a]

	agarsenone (**1**)		agarsenolides			
			major (**2a**)		minor (**2b**)	
position	δ_C[b] type	δ_H[b] (J in Hz)	δ_C[c] type	δ_H[c] (J in Hz)	δ_C[c] type	δ_H[c] (J in Hz)
1	131.4, C		144.9, C		144.7, C	
2	195.5, C		198.5, C[d]		198.5, C[e]	
3α	46.0, CH_2	2.48 d (12.9)	48.9, CH_2	2.69–2.77, m	48.5, CH_2	2.69–2.77, m
3β		1.80–1.95, m		2.27–2.38, m		2.27–2.38, m
4	30.3, CH	1.80–1.95, m	29.9, CH	2.69–2.77, m	29.2, CH	2.69–2.77, m
5α	35.5, CH_2	2.24, d (13.1)	36.4, CH_2	2.85, dd (3.5, 16.0)	35.1, CH_2	3.08, dd (3.1, 15.6)
5β		1.80–1.95, m		2.60, dd (10.6, 16.0)		2.52, dd (10.5, 15.6)
6	146.3, C		142.2, C		141.6, C	
7	117.8, C		124.0, C		124.1, C	
8	156.5, C		155.6, C		155.9, C	
9α	29.2, CH_2	2.64, dd (8.1, 17.1)	113.0, CH	6.89, s[c]	112.9, CH	6.91, s[c]
9β		2.34, dd (1.0, 17.1)				
10	26.9, CH	3.51, m (7.2)	127.5, C		127.7, C	
11	118.4, C		38.1, CH	3.74, q (7.5)	38.0, CH	3.71, q (7.6)
12	140.6, CH	6.81, brs	177.7, C[d]		177.7, C[e]	
13	10.2, CH_3	1.74, d (1.2)	16.1, CH_3	1.61, d (7.5)	16.0, CH_3	1.64, d (7.6)
14	21.3, CH_3	0.69, d (5.6)	21.7, CH_3	1.16, d (6.4)	20.8, CH_3	1.11, d (6.2)
15	18.7, CH_3	1.01, d (7.0)	24.3, CH_3	2.68, s	24.2, CH_3	2.67, s

[a]Data were recorded on a Bruker Avance DPX-400 spectrometer. Chemical shifts: δ values are given in ppm with reference to the signal of $CDCl_3$ (δ 7.26 ppm) or benzene-d_6 (δ 7.16 ppm) and to the center peak of the signal of $CDCl_3$ (δ 77.1 ppm) and of benzene-d_6 (δ 128.0 ppm) for ^{13}C. [b]In benzene-d_6. [c]In $CDCl_3$. [d,e]Overlapped signals.

carbons, one sp^2 methine, two sp^3 methines, three sp^3 methylenes, and three methyls. COSY data allowed the determination of the spin system sequence from H-3 to H-5 and H-14 and from H-9 to H-10 and H-15 and showed a long-range coupling between H-13 and H-15. Further support for this assignment was provided by HMBC correlations observed between H-3α/C-2, H-14/C-3, H-14/C-5, H-9α/C-7, H-9β/C-1, H-9β/C-8, and H-15/C-9 (Figure 1).

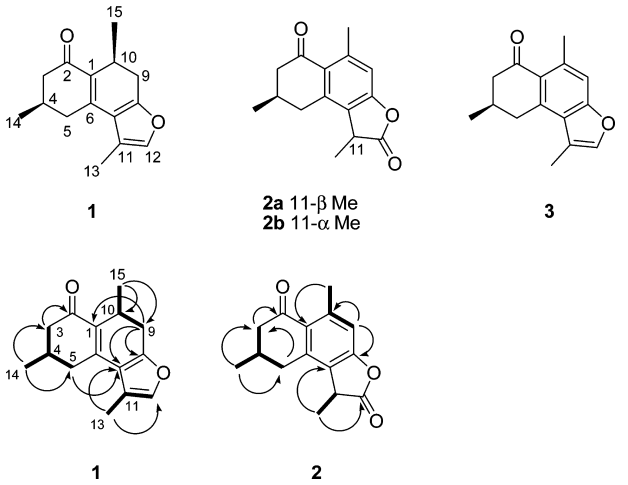

Figure 1. Key COSY (thick bonds) and HMBC (arrows) correlations for **1** and **2**.

The conversion of **1** to **3** in chlorinated solvents provided definitive proof of the furanocadinane skeleton. In **1** the coupling constants between H-9 and H-10 ($J_{9\beta,10}$ < 1 Hz; $J_{9\alpha,10}$ = 8.1 Hz) indicated a dihedral angle of ca. 90° between H-9β and H-10 and close to 40° between H-9α and H-10, due to a quasi-axial orientation of the 15-methyl. H-3α and H-5α appeared in the ^1H NMR spectrum ($CDCl_3$) as a doublet of doublets centered at δ 2.75 and 2.52, respectively. H-3α showed a geminal coupling constant (J = 17.5 Hz) and an axial–equatorial coupling constant with H-4 (J = 4.5 Hz), while H-5α showed a geminal coupling constant (J = 15.8 Hz) and an axial–equatorial coupling constant with H-4 (J = 2.1 Hz). On the other hand, H-3β (δ 2.38) resonated as a doublet of doublets with a geminal constant (J = 17.5 Hz) and a *trans*-diaxial coupling constant with H-4 (J = 10.0 Hz). These values are compatible with an equatorial disposition of the 14-methyl group.

No information about the relative configuration of C-4 and C-10 could be obtained by NOESY experiments (Figure 2). Therefore, a computational analysis of chiroptical properties, i.e., ORD and ECD, of **1** and its degradation product **3** was undertaken in order to ascertain their relative and absolute configurations. Although **3** is a known compound,[9] its absolute configuration remains undefined.

Figure 2. Key NOESY correlations for agarsenone (**1**).

dx.doi.org/10.1021/np400114b | J. Nat. Prod. 2013, 76, 1254–1259

First, the absolute configuration at C-4 of compound (−)-**3** was assigned by comparison between experimental chiroptical data and TDDFT calculations for (4*R*)-**3**. Conformational analysis for (4*R*)-**3** was initially carried out by molecular mechanics calculations to find two conformers having an equatorial and axial C-4 methyl group, respectively. The conformers were fully optimized in the gas phase at the DFT/B3LYP/TZVP level of theory, obtaining relative free energies and Boltzmann population percentages (Figure 3). The

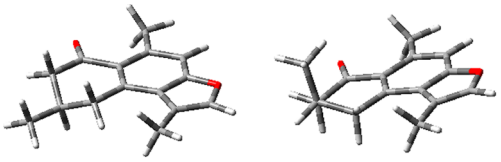

eq (0.00/92.3%) **ax** (1.47/7.7%)

Figure 3. Computed (DFT/B3LYP/TZVP) most stable conformers of (*R*)-**3**. In parentheses Δ*G* (kcal mol^{-1})/population in gas phase.

equatorial conformer was found to be predominant (92.3%). The optical rotation at 589 nm for (*R*)-**3** was then calculated at the TDDFT/B3LYP/aug-cc-pVDZ level[19] using the IEFPCM[20] implicit solvation model for CH_2Cl_2, affording a value of −15.9, in good agreement with the experimental value of $[\alpha]_D$ −19.9 (*c* 0.2, CH_2Cl_2), thus supporting the assignment of the (4*R*)-configuration. Further evidence for this assignment was provided by ECD analysis. The ECD spectrum of (*R*)-**3** was simulated at the TDDFT/CAM-B3LYP/aug-cc-pVDZ level in the gas phase and compared with the experimental data for (−)-**3**.[21] The theoretical ECD spectrum for (*R*)-**3** was in good agreement with the experimental data for (−)-**3** (Figure 4).

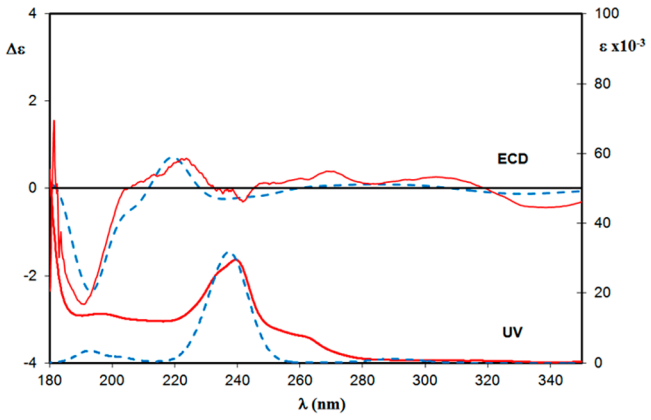

Figure 4. Experimental ECD and UV spectra of (−)-**3** in CH_3CN (solid red line) and calculated (TDDFT/CAM-B3LYP/aug-cc-pVDZ/gas phase) ECD and UV spectra of (*R*)-**3** (dashed blue line). Calculated spectra are red-shifted by 15 nm.

The sequence of experimental Cotton effects (CEs) observed, strongly negative at 190 nm and negative at 335 nm, was satisfactorily reproduced by the calculations in sign, position, and relative intensity. Such analysis unambiguously allows the assignment of the (4*R*) absolute configuration for (−)-**3**. As the transformation of (−)-**1** to (−)-(*R*)-**3** does not involve a change of C-4 configuration, the same (*R*) absolute configuration at this carbon was assumed for (−)-**1**. Therefore, assignment of absolute configuration to (−)-**1** required comparison with chiroptical data computed only for (4*R*,10*S*) and (4*R*,10*R*) diastereoisomers. To assign the C-10 configuration, the ECD spectra of (4*R*,10*S*)-**1** and (4*R*,10*R*)-**1** were computed and compared with experimental data. Conformational analysis for (4*R*,10*S*)-**1** and (4*R*,10*R*)-**1** provided only two conformers for each diastereoisomer. For (4*R*,10*S*)-**1** a *syn* axial−equatorial conformer (96.9%) and a *syn* diaxial conformer (3.1%) were found (Figure 5), while for (4*R*,10*R*)-**1**

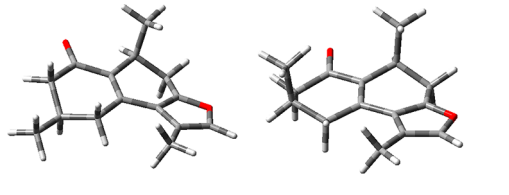

***syn*-ax,eq** (0.00/96.9%) [0.00/96.4%] ***syn*-ax,ax** (2.03/3.1%) [1.95/3.6%]

Figure 5. Computed (DFT/B3LYP/TZVP) most stable conformers of (4*R*,10*S*)-**1**. In parentheses Δ*G* (kcal mol^{-1})/population in gas phase; in square brackets values obtained in the Et_2O IEFPCM solvation model.

calculations provided an *anti* axial−equatorial (91.5%) and an *anti* diaxial (8.5%) conformer (Figure 6). The ECD spectrum

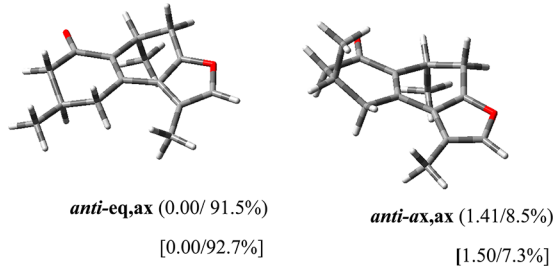

***anti*-eq,ax** (0.00/ 91.5%) [0.00/92.7%] ***anti*-ax,ax** (1.41/8.5%) [1.50/7.3%]

Figure 6. Computed (DFT/B3LYP/TZVP) most stable conformers of (4*R*,10*R*)-**1**. In parentheses Δ*G* (kcal mol^{-1})/population in gas phase; in square brackets values obtained in the Et_2O IEFPCM solvation model.

of (−)-**1** recorded in Et_2O under argon, to prevent its decomposition, showed three main features (Figure 7 and Table 2): a negative CE at 225 nm, a positive CE at 288 nm, and a broad negative band in the 309−400 nm region. The ECD spectra of (4*R*,10*S*)-**1** and (4*R*,10*R*)-**1** were simulated at the TDDFT/CAM-B3LYP/aug-cc-pVDZ level using the IEFPCM[20] implicit solvation model for Et_2O. The computed spectrum of (4*R*,10*S*)-**1** displayed CEs with the same sequence (negative/positive/negative), shape, and relative intensity as the experimental spectrum of (−)-**1**, while the ECD spectrum calculated for (4*R*,10*R*)-**1** was significantly different from the experimental data. These data supported the assignment of the (4*R*,10*S*) absolute configuration to (−)-**1**.

Such an assignment is not definitive because experimental and calculated spectra did not fit perfectly. Calculations carried out with a different long-range-corrected functional such as lc-ωpbe[22] (see Figure S21 in the Supporting Information) did not lead to significant improvement of the spectra agreement (see Supporting Information). Therefore, to further support the above assignment, we attempted to computationally reproduce the ORD curve of (−)-**1**. In fact, it has been shown that in the case of complex molecules the use of more than a single chiroptical technique can provide more reliable results.[23] The

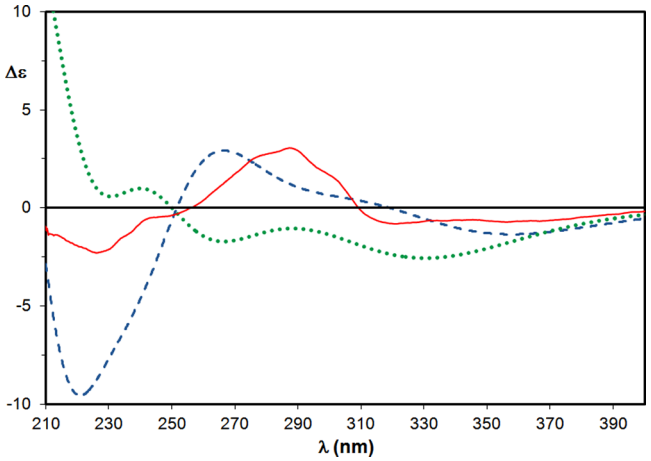

Figure 7. Experimental ECD spectrum of (−)-**1** in Et_2O (solid red line) and calculated (TDDFT/CAM-B3LYP/aug-cc-pVDZ/IEFPCM Et_2O) ECD spectra of (4*R*,10*S*)-**1** (dashed blue line) and (4*R*,10*R*)-**1** (dotted green line). Calculated spectra are red-shifted by 25 nm.

Table 2. Main UV and ECD Features of (−)-3 and (−)-1

compd	UV λ (nm) [$\varepsilon \times 10^{-3}$]	ECD λ (nm) [$\Delta\varepsilon$]
1[a]	232[70.4], 238[68.5], 284[49.6]	225[−2.2], 276sh[+2.5], 288[+3.1], 301sh[+1.5], 318[−0.8]
3[b]	196[29.0], 240[60.0], 260sh[25.0], 310[7.5]	190[−13.3], 222[+3.4], 242[−1.5], 269[+1.9] 335[−2.1]

[a]Spectra recorded in Et_2O (c ~1 × 10^{-3} M). [b]Spectra recorded in MeCN (c ~1 × 10^{-3} M).

optical rotation of (−)-**1** was recorded at several wavelengths in Et_2O, obtaining the ORD curve in Figure 8, which was

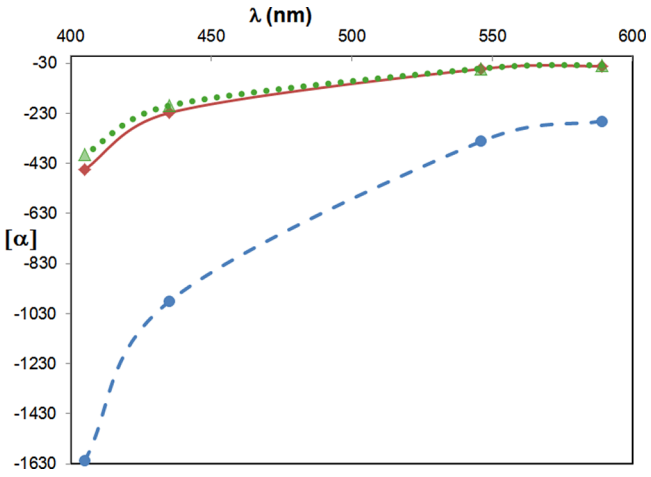

Figure 8. Experimental ORD curve of (−)-**1** in Et_2O (solid red line, ◆) and calculated (TDDFT/B3LYP/aug-cc-pVDZ/IEFPCM Et_2O) ORD curves for (4*R*,10*S*)-**1** (dotted green line, ▲) and (4*R*,10*R*)-**1** (dashed blue line, ●).

compared with ORD curves calculated for (4*R*,10*S*)-**1** and (4*R*,10*R*)-**1** diastereoisomers. ORD calculations were performed at the TDDFT/B3LYP/aug-cc-pVDZ level on geometries obtained at the DFT/B3LYP/TZVP level, performing both calculations in an Et_2O implicit IEFPCM solvation model.[20] As shown in Figure 8 the calculated ORD curve for (4*R*,10*S*)-**1** fits very well with experimental data, while the ORD calculation for (4*R*,10*R*)-**1** provided values about five times higher than experimental ones (Table 3). This result further confirmed the assignment of a (4*R*,10*S*) absolute configuration for (−)-**1**.

Table 3. Comparison of Experimental and Calculated Optical Rotations for 1

	experimental optical rotations[a]	calculated optical rotations[b]	
wavelength (nm)	(−)-**1**	(4*R*,10*S*)-**1**	(4*R*,10*R*)-**1**
589	−40.4	−36.3	−260.7
546	−52.0	−50.4	−341.6
435	−227.6	−198.6	−980.9
405	−453.2	−394.0	−1616.6

[a]Optical rotations recorded in Et_2O (c 0.25 g/100 mL). [b]Optical rotations obtained as Boltzmann averages calculated at the TDDFT/B3LYP/aug-cc-pVDZ level employing the Et_2O implicit IEFPCM solvation model.

Agarsenolides A and B (**2a** and **2b**, respectively) were obtained as an inseparable mixture of isomers (ratio 2.4:1) by autoxidation of agarsenone (**1**).[24] All attempts to separate the mixture failed, leading to the decomposition of the compounds; therefore the mixture was subjected to structure elucidation. The molecular formula of both isomers was established to be $C_{15}H_{16}O_3$ by HRMS, indicating eight indices of hydrogen deficiency. The ^{13}C NMR spectrum of the mixture (Table 1), supported by a JMODXH experiment, showed the presence of three methyls, two aliphatic methylenes, and two aliphatic methines. In the sp^2 region, we observed one methine, five quaternary carbons, and two carbonyls. The ^{13}C NMR spectroscopic data of the dihydronaphthalenone core were similar to those of **3**.[10]

The significant differences were the replacement of the olefinic carbon at C-11 with an aliphatic methine resonating at δ 38.1/38.0 (δ_H 3.74/3.71, q, J = 7.5/7.6 Hz) and the presence of a second carbonyl at δ 177.7. The presence of the β-methyl lactone was evidenced by the resonances at δ 177.7 (C-12), 124.0/124.1 (C-7), 155.6/155.9 (C-8), 38.1/38.0 (C-11), and 16.1/16.0 (C-13)[25] and by the absorbance at 1807 cm^{-1} in the IR spectrum. The peaks at δ 113.0/112.9 (C-9), 127.5/127.7 (C-10), and 24.3/24.2 (C-15) were indicative of the presence of the methyl-substituted aromatic ring. The connections from C-3 to C-5 and between C-11 and C-13 were confirmed by COSY data. All these features were characteristic of the presence of a 2,3-dihydrobenzo[*b*]furan-2-one system. HMBC correlations permitted establishment of the structure of **2** as depicted in Figure 1. Particularly diagnostic were correlations between H-3/C2, H-14/C4 and C5, H-5/C4 and C6, H-9/C8, C10, and C15, H-11/C7, C12, and C13, and H-15/C1, C9, and C10. The relative configurations of **2a** and **2b** were determined by analysis of NOESY data and comparison with **1**'s NMR data (Figure 9). The absolute configuration at C-4 was assigned as *R*, the same as agarsenone **1**, from which these compounds arise by decomposition. From all these observations we assigned a β-orientation of the C-11 methyl group in **2a** and α in **2b**.

CONCLUSION

We reported the isolation and structure identification of agarsenone (**1**), a new furanosesquiterpenoid that can easily decompose during extraction and purification to give myrrhone (**3**) and, by autoxidation, agarsenolides (**2a** and **2b**). The

dx.doi.org/10.1021/np400114b | J. Nat. Prod. 2013, 76, 1254−1259

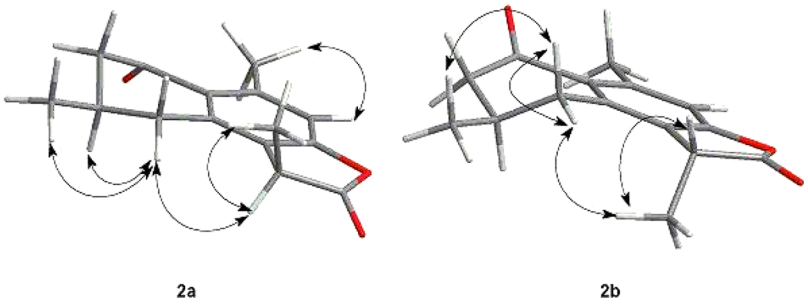

Figure 9. Key NOESY correlations for agarsenolides (**2a** and **2b**).

structures of **1**−**3** were elucidated by NMR methods, and their relative and absolute configurations were determined by TDDFT computational simulation of ORD and ECD spectra. This study provides the first assignment of absolute configuration for bioactive compounds from myrrh. Moreover, our observations may suggest that, in certain cases, myrrhone, a well-known compound found in *Commiphora* spp. myrrh extracts,[26] could be an experimental artifact and not a genuine plant metabolite.

EXPERIMENTAL SECTION

General Experimental Procedures. Optical rotations were measured with a JASCO DIP-1000 digital polarimeter. Absorption and ECD spectra were recorded at room temperature on a JASCO J815 spectropolarimeter, using 0.5 mm cells and concentrations of about 1×10^{-3} M in MeCN for (−)-**3** and in Et_2O for (−)-**1**. IR spectra were recorded on a JASCO 410 spectrophotometer equipped with a diffuse reflectance accessory. High-resolution MS spectra were acquired on a Q-TOF Premier instrument (Waters, Milford, MA, USA), equipped with a nanospray ion source and provided with a lock-mass apparatus to perform a real-time calibration correction. GC analyses (Table S2) were performed on a Hewlett-Packard HP 6890 gas chromatograph equipped with a Hewlett-Packard MS 5973 mass selective detector and a fused silica capillary column (HP-5MS; 30 m × 0.25 mm i.d., 0.25 μm film thickness). NMR spectra were recorded using a Bruker Avance DPX-400 spectrometer operating at frequencies of 400 MHz (^{1}H) and 100 MHz (^{13}C) and a Bruker DRX-600 spectrometer operating at 600 MHz (^{1}H) and 150.85 MHz (^{13}C). The spectra were measured in $CDCl_3$ and C_6D_6. The ^{1}H and ^{13}C NMR chemical shifts (δ) were expressed in ppm with reference to the solvent signals [$CDCl_3$ δ_H 7.26 and δ_C 77.1, C_6D_6 δ_H 7.16 and δ_C 128.0]. Column chromatography was performed using Davisil LC60A 60−200 μm silica gel. Fractions were monitored by TLC (silica gel 60 F_{254}, Merck), and spots on TLC were visualized under UV light and after staining with *p*-anisaldehyde−H_2SO_4−EtOH (1:1:98) followed by heating at 110 °C. For preparative TLC silica gel 60 F_{254} plates (Merck) were used, and the compounds visualized by UV.

Plant Material. The resin of *Commiphora erythraea* (Agarsu grade I) commercialized by Agarsu Liben Cooperative and imported into Italy by IPO (Increasing People Opportunities) Association (www.ipoassociazione.org) was studied. A voucher specimen (#MCM-1) of the resin (Agarsu grade I) is deposited at the Dipartimento di Chimica e Tecnologia del Farmaco-Sez. Chimica Organica, University of Perugia.

Extraction and Isolation. The ground resin (15 g) was extracted by maceration in MeOH (3 × 250 mL) at room temperature for 24 h. After filtration, the organic solutions were concentrated at 40 °C to give the MeOH extract (7.52 g). The extract was divided into two fractions by column chromatography (SiO_2) using *n*-hexane for the elution of fraction M1 (0.42 g) and Et_2O for the elution of fraction M2 (6.19 g). An aliquot of the M2 fraction (3.5 g) was purified on a SiO_2 gel chromatography column using a gradient of *n*-hexane−Et_2O (0−100%), collecting 7 mL fractions that were evaluated by TLC and combined upon similar appearance, yielding 31 fractions (Fr1−Fr31). Composition and amounts of the fractions are reported in Table 1S (Supporting Informations).

Fr22 (65 mg) was further purified by preparative TLC (elution with *n*-hexane−Et_2O 25%), affording agarsenone (**1**) (34 mg) and *rel*-1*S**,2*S**-epoxy-4*R*-furanogermacr-10(15)-en-6-one (**10**) (15 mg).

*Agarsenone (**1**):* colorless oil; $[\alpha]^{22}_D$ −78.3 (*c* 0.64 in TBME); $[\alpha]^{26}_D$ −30.6 (*c* 1.10, benzene); FT-IR ν_{max} 2956, 1762, 1652, 1549 cm^{-1}; ^{1}H NMR ($CDCl_3$, 400 MHz) δ 0.91 (3H, d, *J* = 7.0 Hz, H-14), 1.11 (3H, d, *J* = 6.3 Hz, H-15), 2.15 (3H, brs, H-13), 2.20−2.30 (3H, m, H4, H-5β), 2.38 (1H, dd, *J* = 10.0, 17.5 Hz, H-3β), 2.52 (1H, dd, *J* = 2.1, 15.8 Hz, H-5α), 2.54 (1H, d, *J* = 17.0 Hz, H-9α), 2.75 (1H, dd, *J* = 4.5, 17.5 Hz, H-3α), 2.86 (1H, dd, *J* = 7.7, 17.0 Hz, H-9β), 3.30 (1H, m, *J* = 7.7 Hz, H-10), 7.11 (1H, brs, H-12); ^{1}H NMR and ^{13}C NMR in benzene-d_6 see Table 1; $C_{15}H_{18}O_2$ HREIMS *m*/*z* 231.1367 [M + H]$^+$, calcd 213.1385.

*Agarsenolides (**2a** and **2b**):* yellowish oil; FT-IR ν_{max} 2953, 1807, 1676, 1587, 1451 cm^{-1}; ^{1}H and ^{13}C NMR see Table 1; HREIMS *m*/*z* 245.1158 [M + H]$^+$, calcd 245.1178.

*Myrrhone (**3**):* colorless oil; $[\alpha]^{24}_D$ −19.9 (*c* 0.2, CH_2Cl_2); FT-IR, ^{1}H and ^{13}C NMR were in agreement with reported data.[9,10]

Computational Details. Preliminary conformational analyses were performed by the Spartan02 package[27] employing MMFF94s molecular mechanics force field with Monte Carlo searching and fixing arbitrarily assigned absolute configurations (*R*) for **3** and (4*R*,10*S*) and (4*R*,10*R*) for **1**. All possible conformers were searched, considering the degrees of freedom of the system, retaining only the structures within an energy range of 30 kcal/mol with respect to the most stable one. The minimum energy conformers found by molecular mechanics were further fully optimized by using the DFT at the DFT/B3LYP/TZVP level in either the gas phase or solvent with the IEFPCM implicit solvation model,[20] as implemented in the Gaussian09 package.[28] For each compound two conformers were found (Figures 3, 5, and 6). All conformers are real minima, no imaginary vibrational frequencies have been found, and the free energy values have been calculated and used to get the Boltzmann population of conformers at 298.15 K. Optical rotations were computed by using the TDDFT/B3LYP/aug-cc-pVDZ level on the DFT-optimized geometries. Solvent effects were modeled with the IEFPCM implicit solvation model[20] with parameters of Et_2O for **1** and CH_2Cl_2 for **3**. The DFT/B3LYP/TZVP geometries were also employed as input geometries for calculation of UV and ECD spectra at the TDDFT/CAM-B3LYP/aug-cc-pVDZ level. TDDFT calculations employing the long-range corrected CAM-B3LYP functional[29] provided a good reproduction of Cotton effects observed in the theoretical ECD spectra. The theoretical ORD, UV, and ECD spectra were obtained as averages over the conformers' Boltzmann populations. The ECD spectra were obtained from calculated excitation energies and rotational strengths, as a sum of Gaussian functions centered at the wavelength of each transition, with a parameter σ (width of the band at half-height) of 0.5 eV for **1** and 0.3 eV for **3**. To guarantee origin independence and to evaluate the quality of the molecular wave functions employed,[30] theoretical ECD spectra were obtained in both the length and velocity representation, using the lowest 30 states. The velocity/length calculated spectra were almost coincident, indicating a good level of calculation. Therefore, in all figures only the velocity-form predicted spectra are reported. UV and

ECD calculations provided electronic transitions at slightly higher energy than experimental; therefore, for a clearer comparison with experimental data in Figures 4 and 7, calculated UV and ECD spectra of **3** and **1** have been red-shifted by 15 and 25 nm, respectively.

■ ASSOCIATED CONTENT

Supporting Information

Purification details, NMR spectra of the described compounds, conformational analysis, and ECD data of **1** and **3** are available free of charge via the Internet at http://pubs.acs.org.

■ AUTHOR INFORMATION

Corresponding Author

*(M.C.M.) Tel: +39-075-585-5104. Fax: +39-075-585-5116. E-mail: marcotu@unipg.it or mariacarla.marcotullio@unipg.it. (S.S.) Tel: +39-0971-20-6098. Fax: +39-0971-20-5678. E-mail: stefano.superchi@unibas.it.

Present Address

[§]Department of Organic Chemistry, Arrhenius Laboratory, Stockholm University, SE-106 91 Stockholm, Sweden.

Notes

The authors declare no competing financial interest.

■ ACKNOWLEDGMENTS

The authors wish to thank Fondazione Cassa di Risparmio (Project Code: 2010.011.0410), Università della Basilicata (R.I.L. 2010 grant), and MIUR (Rome) (PRIN project 2008LYSESR) for financial support, Ipoassociazione, Agarsu Liben Cooperative for providing the resin, and Infarmazone. We thank Prof. L. Rastrelli (Università di Salerno) for the use of HRMS and Bruker 600 MHz facilities. A. Palmier OLJ BPharm (Hons) Melit. (University of Malta) and M. Kerrigan MA (Cantab) are gratefully acknowledged for valuable linguistic suggestions.

■ REFERENCES

(1) Zorloni, A. MD Dissertation, University of Pretoria, Pretoria, South Africa, 2007.

(2) Maradufu, A. *Phytochemistry* **1982**, *21*, 677−680.

(3) Carroll, J. F.; Maradafu, A.; Warthen, J. D. *Entomol. Exp. Appl.* **1989**, *53*, 111−116.

(4) Marcotullio, M. C.; Santi, C.; Oball-Mond Mwankie, G. N.; Curini, M. *Nat. Prod. Commun.* **2009**, *4*, 1751−1754.

(5) Fraternale, D.; Sosa, S.; Ricci, D.; Genovese, S.; Messina, F.; Tomasini, S.; Montanari, F.; Marcotullio, M. C. *Fitoterapia* **2011**, *82*, 654−661.

(6) GC-MS analysis of these oils and extracts revealed the presence of a compound with retention index (RI) of 1894 on a HP-5MS column (ref 4). Every attempt to isolate it failed. After chromatographic purification using methylene chloride it could not be detected anymore. Conversely, myrrhone (**3**) was either not present or present only in traces in the starting oil/extract (refs 4 and 5).

(7) Dekebo, A.; Dagne, E.; Sterner, O. *Fitoterapia* **2002**, *73*, 48−55.

(8) Hikino, H.; Konno, C.; Takemoto, T.; Tori, K.; Ohtsuru, M.; Horibe, I. *Chem. Commun.* **1969**, 662−663.

(9) Barreira, E. S.; Quieroz Monte, F. J.; Braz-Filho, R. *Nat. Prod. Lett.* **1996**, *8*, 285−289.

(10) Zhu, N.; Sheng, S.; Rosen, R. T.; Ho, C.-T. *Flav. Frag. J.* **2003**, *18*, 282−285.

(11) König, W. A.; Bülow, N.; Fricke, C.; Melching, S.; Rieck, A.; Muhle, H. *Phytochemistry* **1996**, *4*, 629−633.

(12) Marcotullio, M. C.; Messina, F.; Curini, M.; Macchiarulo, A.; Cellanetti, M.; Ricci, D.; Giamperi, L.; Bucchini, A.; Minelli, A.; Mierla, A. L.; Bellezza, I. *Molecules* **2011**, *16*, 10357−10369.

(13) Cenci, E.; Messina, F.; Rossi, E.; Epifano, F.; Marcotullio, M. C. *Nat. Prod. Commun.* **2012**, *7*, 143−144.

(14) Brieskorn, C. H.; Noble, P. *Phytochemistry* **1983**, *22*, 187−189.

(15) Zhu, N.; Kikuzaki, H.; Sheng, S.; Sang, S.; Rafi, M. M.; Wang, M.; Nakatani, N.; DiPaola, R. S.; Rosen, R. T.; Ho, C.-T. *J. Nat. Prod.* **2001**, *64*, 1460−1462.

(16) For general discussion of the *ab initio* calculation of chiroptical properties: (a) Autschbach, J.; Nitsch-Velasquez, L.; Rudolph, M. *Top. Curr. Chem.* **2011**, *298*, 1−98. (b) Stephens, P. J. *Computational Medicinal Chemistry for Drug Discovery*; Bultnick, P., de Winter, H., Langenaecker, W., Tollenaere, J., Eds.; Dekker: New York, NY, 2003; pp 699−725. (c) Autschbach, J. *Chirality* **2009**, *21*, E116−E152.

(17) Autoxidation of **1** could occur through a hetero-Diels-Alder reaction between oxygen and a furan, followed by hydrolysis and acid (from chlorinated solvent decomposition)-catalyzed dehydration into the stable benzofuran. See for example: Chen, K.-S.; Wu, Y.-C. *Tetrahedron* **1999**, *55*, 1353−1366.

(18) Bigler, P. *NMR Spectroscopy*; Wiley: Weinheim, 2000; p 57.

(19) (a) Becke, A. D. *J. Chem. Phys.* **1993**, *98*, 5648−5652. (b) Lee, C.; Yang, W.; Parr, R. G. *Phys. Rev. B* **1988**, *37*, 785−789. (c) Stephens, P. J.; Devlin, F. J.; Chabalowski, C. F.; Frisch, M. J. *J. Phys. Chem.* **1994**, *98*, 11623−11627.

(20) Tomasi, J.; Mennucci, B.; Cammi, R. *Chem. Rev.* **2005**, *105*, 2999−3094.

(21) (a) For synthetic compounds: Xu, D.-Q.; Wang, Y.-F.; Luo, S.-P.; Zhang, S.; Zhong, A.-G.; Chen, H.; Xu, Z.-Y. *Adv. Synth. Catal.* **2008**, *350*, 2610−2616. (b) For natural products: Evidente, A.; Superchi, S.; Cimmino, A.; Mazzeo, G.; Mugnai, L.; Rubiales, D.; Andolfi, A.; Villegas-Fernández, A. M. *Eur. J. Org. Chem.* **2011**, 5564−5570.

(22) Vydrov, O. A.; Scuseria, G. E. *J. Chem. Phys.* **2006**, *125*, 234109−234117.

(23) See for example: Mazzeo, G.; Santoro, E.; Andolfi, A.; Cimmino, A.; Troselj, P.; Petrovic, A. G.; Superchi, S.; Evidente, A.; Berova, N. *J. Nat. Prod.* **2013**, *76*, 588−599.

(24) Ulubelen, A.; Oksuz, S. *J. Nat. Prod.* **1984**, *47*, 177−178.

(25) Harrowven, D. C.; Lucasa, M. C.; Howes, P. D. *Tetrahedron* **2001**, *57*, 791−804.

(26) (a) Shen, T.; Wan, W.; Yuan, H.; Kong, F.; Guo, H.; Fan, P.; Lou, H. *Phytochemistry* **2007**, *68*, 1331−1337. (b) Shen, T.; Wan, W.-Z.; Wang, X.-N.; Yuan, H.-Q.; Ji, M.; Lou, H.-X. *Helv. Chim. Acta* **2009**, *92*, 645−652.

(27) *SPARTAN '02*; Wavefunction Inc.: Irvine, CA; http://www.wavefunction.com.

(28) Frisch, M. J.; et al. *Gaussian 09*, Revision A.02; Gaussian, Inc.: Wallingford, CT, 2009.

(29) Yanai, T.; Tew, D. P.; Handy, N. C. *Chem. Phys. Lett.* **2004**, *393*, 51−57.

(30) Moscowitz, A. In *Modern Quantum Chemistry*; Sinanoglu, O., Ed.; Academic Press: London, 1965; Part III, p 31.